Optical hyperparametric oscillations in a whispering-gallery-mode resonator: Threshold and phase diffusion

Andrey B. Matsko, Anatoliy A. Savchenkov, Dmitry Strekalov, Vladimir S. Ilchenko, and Lute Maleki
Jet Propulsion Laboratory, California Institute of Technology, 4800 Oak Grove Drive, Pasadena, California 91109-8099, USA
(Received 10 August 2004; published 8 March 2005)

We present a theoretical analysis of optical parametric oscillations through four-wave mixing in a nonlinear high-*Q* whispering-gallery-mode resonator. It is shown that even a small flux of pump photons is sufficient to reach the threshold of the oscillations. We demonstrate that due to narrow bandwidth of the resonator modes as well as the high efficiency of the resonant frequency conversion the oscillator produces a stable narrow-band beat note of the pump, signal, and idler waves making an all-optical secondary frequency reference feasible.

DOI: 10.1103/PhysRevA.71.033804 PACS number(s): 42.60.Da, 42.65.Ky, 42.65.Hw, 42.65.Yj

I. INTRODUCTION

Hyperparametric optical oscillation [1], also known in fiber optics as modulation instability [2], is based on four-wave mixing (FWM) among two pump, signal, and idler photons, and results in the growth of the signal and idler optical sidebands from vacuum fluctuations at the expense of the pumping wave. The hyperparametric oscillations are different from the parametric ones. The parametric oscillations (i) are based on $\chi^{(2)}$ nonlinearity coupling three photons, and (ii) have phase matching conditions involving far separated optical frequencies, that can only be satisfied in birefringent materials in the forward direction. In contrast, the hyperparametric oscillations (i) are based on $\chi^{(3)}$ nonlinearity coupling four photons, and (ii) have phase matching conditions involving nearly degenerate optical frequencies that can be satisfied in most materials both in the forward and backward directions.

Observations of hyperparametric oscillations in transparent solids are hindered by the small nonlinearity of the materials, so the oscillations are usually observed with pulsed pumping light, to increase optical intensity, and with optical fibers, to increase the interaction length [2,3]. A significant reduction of the oscillation threshold is possible by means of various resonant structures. The use of a cavity could substantially enhance the efficiency of the FWM process resulting in the observation of oscillations in the continuous wave (cw) regime [4]. Oscillations have also been observed in atomic vapor cells placed in optical resonators [5–8]. Ultralow threshold mirrorless cw hyperparametric oscillations were obtained in multilevel coherent media [9], where the medium itself played the role of the resonator. Recently, the study of hyperparametric oscillations had an interesting twist connected with the development of whispering-gallery-mode (WGM) as well as photonic crystal [10,11] microresonator technology.

The oscillations occurring in cavities or cavitylike systems filled with transparent solids were analyzed theoretically, e.g., in isotropic photonic crystals [12], and were observed experimentally in crystalline WGM resonators [13,14]. It was suggested, in particular, that the narrow-band beat-note signal between the optical pump and the generated sidebands emerging from a high-*Q* WGM resonator could be used as a secondary frequency reference [14].

The hyperparametric oscillations involving an atomic system placed into a cavity (e.g., Ref. [5]) and oscillations occurring in an optical cavity filled with a transparent nonlinear Kerr medium [13,14] have certain differences. For instance, in the first case, the oscillation frequency is given by both the frequency of the atomic two-photon Raman transition and the resonator mode structure, while in the second case it is determined by the resonator mode structure only. On the other hand, the mathematical description of both processes is similar because they both are based on the four-wave mixing. The nonlinear resonators can be considered "artificial atoms," like semiconductor quantum dots. This is especially true for open high-*Q* microresonators made of dispersive nonlinear dielectrics because modes of the resonators are substantially nonequidistant and resonantly enhanced nonlinearities are high.

Here we theoretically study hyperparametric oscillations in a nonlinear ring, e.g., WGM resonator, primarily focusing on the properties of the beat-note signal produced by mixing the optical pump and the generated sidebands on a fast photodiode. For a resonator with gigahertzs difference between frequencies of the neighboring resonator modes belonging to the same mode family [the free spectral range (FSR)], this beat note signal is at microwave frequencies. We show that the beat-note signal depends on the FSR frequency of the resonator. We found that the beat note does not experience a frequency shift due to the self- and cross-phase modulation effects because of the intrinsic symmetry of the FWM process in the resonator

The phase stability of the signal increases with increase of the *Q* factor of the resonator modes for the same given value of the pump power. There exists a maximum of the phase stability (minimum of the phase diffusion) of the beat-note signal that does not depend either on the pump power or *Q* factor of the modes. Keeping in mind that WGM's *Q* factor can exceed 10^{10} (a few tens of kilohertz resonance linewidth) [15], we find the Allan deviation factor of the oscillations to be smaller than 10^{-12} $s^{-1/2}$ for sub-mW optical pumping. The pump threshold could reach mW levels for reasonable experimental parameters.

This paper is organized as follows: In Sec. II we introduce the basic equations. In Sec. III we discuss the steady-state

solution of the equations for expectation values and find the oscillation threshold. In Sec. IV we study phase diffusion of the generated microwave signal. In Sec. V we discuss similarities and differences in the cavity-based and atomic media based oscillators. Calculation details are presented in the Appendixes.

II. BASIC EQUATIONS

Optical oscillations could occur in an optical fiber or in a resonator that is filled with a medium possessing Kerr nonlinearity [2]. The nonlinearity results in a four-photon process like $\hbar\omega_0+\hbar\omega_0 \rightarrow \hbar\omega_1+\hbar\omega_2$, also known as a hyperparametric process, which leads to generation of coherent optical signals from vacuum fluctuations at frequencies ω_1 and ω_2. Generally, in a resonator the following relationships hold: $\omega_1 \approx \omega_0+\omega_{FSR}$ and $\omega_2 \approx \omega_0-\omega_{FSR}$, where ω_0 is the frequency of the external pumping wave in resonance with one of the resonator's modes, and ω_{FSR} stands for the FSR frequency interval of the resonator. A further increase of the optical pumping power and appropriate phase matching conditions could result in the generation of numerous sidebands; however, for the sake of simplicity, we restrict our consideration to three modes.

Langevin equations for the slow amplitude operators A, B_+, and B_- of the intracavity fields can be presented in the form (see Appendix A)

$$\dot{A} = -\Gamma_0 A + ig[A^\dagger A + 2B_+^\dagger B_+ + 2B_-^\dagger B_-]A + 2igA^\dagger B_+ B_- + F_0 + F_{c0}, \tag{1}$$

$$\dot{B}_+ = -\Gamma_+ B_+ + ig[2A^\dagger A + B_+^\dagger B_+ + 2B_-^\dagger B_-]B_+ + igB_-^\dagger AA + F_+ + F_{c+}, \tag{2}$$

$$\dot{B}_- = -\Gamma_- B_- + ig[2A^\dagger A + 2B_+^\dagger B_+ + B_-^\dagger B_-]B_- + igB_+^\dagger AA + F_- + F_{c-}, \tag{3}$$

where

$$\Gamma_0 = i(\omega_0 - \omega + \kappa_0(T)) + \gamma_0 + \gamma_{c0},$$

$$\Gamma_+ = i(\omega_+ - \tilde{\omega}_+ + \kappa_+(T)) + \gamma_+ + \gamma_{c+},$$

$$\Gamma_- = i(\omega_- - \tilde{\omega}_- + \kappa_-(T)) + \gamma_- + \gamma_{c-}.$$

ω_0, ω_+, and ω_- are the eigenfrequencies of the optical cavity modes; γ_0, γ_+, and γ_- are the internal decay rates of the modes; γ_{c0}, γ_{c+}, and γ_{c-} are the decay rates due to external coupling; ω is the carrier frequency of the external pump (A), $\tilde{\omega}_+$ and $\tilde{\omega}_-$ are the carrier frequencies of generated light (B_+ and B_-, respectively). These frequencies are determined by the oscillation process and cannot be controlled externally. However, there is a ratio between them (energy conservation law):

$$2\omega = \tilde{\omega}_+ + \tilde{\omega}_-. \tag{4}$$

Coefficient $\kappa_k(T)$ describes the frequency shift of the mode k due to the temperature change. This coefficient should be taken into account because absorption of the pump and the generated light results in a change of the resonator temperature. Because the modes are confined nearly in the same geometrical volume, the thermal frequency shift is nearly the same for all the modes.

Thermal nonlinearity is important in high-Q WGM resonators [15–18]. For instance, because of the thermal nonlinearity, the trace of the resonance on the screen of oscilloscope changes depending on the laser power and the speed and direction of the laser scan, i.e., coefficient $\kappa(T)$ generally depends on time if external conditions vary. The dependence can be described with two intrinsic relaxation time constants, one of which is responsible for flow of heat from the mode volume to the rest of the resonator, and the other for heat exchange between the resonator and the external environment. To reduce the influence of nonlinearity on the measurement results, the laser scan should be either fast compared with the relaxation constants and the light power must be small, or the temperature shift should be compensated by introducing electronic feedback into the system that tunes the laser frequency with the mode shift [14]. In the latter case $\kappa(T)$ reaches a steady-state value and can efficiently be considered as a constant.

Thermal dependence of the index of refraction for transparent crystals and fused silica can significantly exceed the frequency shift due to self- and cross-phase modulation effects induced by the electronic nonlinearity of the material. For example, for a calcium fluoride resonator $\kappa_m(T) = \omega_m n_0^{-1} \partial n/\partial T \simeq \omega_m \times 10^{-5}\ \mathrm{K}^{-1}$ (ω_m is the resonant frequency of a mode). This frequency shift is five orders of magnitude larger than the width of the resonance if $Q = 10^{10}$ for a single degree of temperature change. This shift generally does not lead to the saturation of the FWM process because it mildly changes the free spectral range of the resonator: $\delta_{FSR}(T) = \omega_{FSR} n_0^{-1} \partial n/\partial T \simeq \omega_{FSR} \times 10^{-5}\ \mathrm{K}^{-1}$, and barely changes the behavior of the beat note of the pump and sidebands. Because FSR depends on temperature, the temperature can be used to tune the oscillator frequency.

Dimensionless slowly varying annihilation operators A, B_+, and B_- in Eqs. (1)–(3) are normalized such that average $|\langle A^\dagger A\rangle|$, $|\langle B_+^\dagger B_+\rangle|$, and $|\langle B_-^\dagger B_-\rangle|$ describe average photon number in the corresponding modes,

$$g = \omega_0 \frac{n_2}{n_0} \frac{\hbar\omega_0 c}{\mathcal{V} n_0}, \tag{5}$$

is a coupling constant, n_2 is an optical constant that characterizes the strength of the optical nonlinearity, n_0 is the linear refractive index of the material, $\mathcal{V}$ is the mode volume, and c is the speed of light in the vacuum.

Langevin force F_{c0} stands for the external pumping of the system with nonzero expectation value

$$\langle F_{c0}\rangle = \sqrt{\frac{2\gamma_{c0} P_0}{\hbar\omega_0}}, \tag{6}$$

where P_0 is the pump power of the mode applied from the outside. Expectation values of the other forces are equal to zero. All the forces are uncorrelated. Commutation relations for them are $[F_j(t), F_j^\dagger(t')] = 2\gamma_j \delta(t-t')$.

The amplitudes of the fields leaving the system could be obtained from

$$A_{out} = \sqrt{2\gamma_{c0}\hbar\omega_0}\left(A - \frac{F_{c0}}{2\gamma_{c0}}\right), \tag{7}$$

$$B_{\pm out} = \sqrt{2\gamma_{c\pm}\hbar\omega_{\pm}}\left(B_{\pm} - \frac{F_{c\pm}}{2\gamma_{c\pm}}\right), \tag{8}$$

where $A^{\dagger}_{out}A_{out}$ ($B^{\dagger}_{\pm\ out}B_{\pm\ out}$) describes power of the carrier (sidebands) exiting the resonator.

III. SOLUTION: EXPECTATION VALUES

Solving Eqs. (1)–(3) in steady state (see Appendix B), keeping expectation values only, and assuming that the modes are identical, i.e., $\gamma_+ + \gamma_{c+} = \gamma_- + \gamma_{c-} = \gamma_0 + \gamma_{c0}$, which is justified by observation with actual resonators, we find the oscillation frequency for generated fields,

$$\omega - \tilde{\omega}_- = \tilde{\omega}_+ - \omega = \frac{1}{2}(\omega_+ - \omega_-), \tag{9}$$

i.e., the beat-note frequency depends solely on the frequency difference between the resonator modes (FSR frequency) and does not depend on the light power, or the laser detuning from the pumping mode. This result shows an advantage of our oscillator over the oscillator based on atomic coherence, e.g., where the oscillation frequency depends on the ac-Stark shift (pump power) [19].

Threshold optical power can be found from the steady-state solution of set (1)–(3),

$$P_{th} \simeq 1.54\ \frac{\pi}{2}\frac{\gamma_0 + \gamma_{c0}}{2\gamma_{c0}}\frac{n_0^2\mathcal{V}}{n_2\lambda Q^2}, \tag{10}$$

where the numerical factor 1.54 comes from the influence of the self-phase modulation effects on the oscillation threshold. The threshold value for a CaF_2 resonator is $P_{th} \approx 0.3$mW, where $n_0 = 1.44$ is the refractive index of the material, $n_2 = 3.2 \times 10^{-16}$ cm^2/W is the nonlinearity coefficient for calcium fluoride, $\mathcal{V} \approx 10^{-4}$ cm^3 is the mode volume, $Q = \omega_0/2(\gamma_0 + \gamma_{c0}) = 6 \times 10^9$, $\gamma_0 = \gamma_{c0}$, and $\lambda = 1.32$ μm. Nearly the same estimations are valid for fused silica resonators.

We solve Eqs. (1)–(3) numerically and evaluate the dependencies of the output pump and a sideband power on the value of the input pump power, focusing on two particular cases of an ideal (or overcoupled) resonator $\gamma_0 = 0$ ($\gamma_{c0} \gg \gamma_0$), and critically coupled resonator $\gamma_0 = \gamma_{c0}$.

For the overcoupled resonator the sum of the powers of the sidebands and the pump leaving the resonator is always conserved: $P_{A\ out} + P_{B+\ out} + P_{B-\ out} = P_0$. The dependencies of the values of the powers on the pump power are presented in Fig. 1. Here and in what follows the value of the pump ($P_{A\ out}$) as well as sideband ($P_{B\ out}$) power is shown normalized with the value of the input pump power (P_0). The input pump power is shown normalized with the oscillation threshold power (P_{th}).

As is shown in Appendix B, the value of the detuning of the carrier frequency of the pump from the frequency of the corresponding resonator mode cannot be varied arbitrarily. The detuning allows us to compensate for the frequency shift of the mode due to self- and cross-phase modulation effects. The smallest possible detuning, when the oscillations still exist, is equal to $\omega_0 - \omega + \kappa(T) \simeq 1.733(\gamma_{c0} + \gamma_c)$.

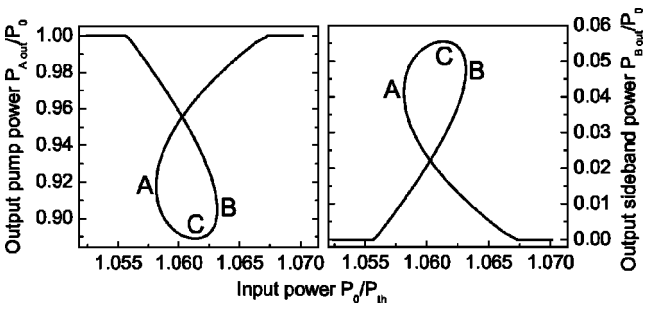

FIG. 1. Dependence of the pump (left) and a sideband (right) power on the input pump power for the case of identical resonator modes and pump frequency such that $\omega_0 - \omega + \kappa(T) = 1.8\gamma_{c0}$. Stable oscillations occur in the region confined between points *A* and *B* (point *C* shows the center of the region).

To study the stability of the system we note that small initial perturbations of all parameters of a stable oscillator should decrease in time. We find eigenvalues of equations that describe the time evolution of the fluctuations of the system [see Appendix C, Eqs. (C1)–(C6)]. The oscillations are stable in the region of parameters where all the eigenvalues correspond to the solutions decreasing in time. This region is located between points *A* and *B* on our plots (see Fig. 1 and following figures). It is worth noting that the stability conditions are different from those for a resonator with internal pumping.

Let us now consider the FWM process in a critically coupled resonator and compare it with the process in an overcoupled resonator. We assume that the loaded *Q* factor as well as the other parameters of the modes stay the same in both cases, with the exception of the ratio between the values of the transmission and absorption rates. We found that the sideband power decreases four times for the critically coupled resonator compared with the case of overcoupled resonator (see Fig. 2), though the functional shape of the dependence is the same in both cases. The transmission curve for the pump light changes compared to the overcoupled system (see Fig. 3). The difference arises because a significant amount of the pump as well as sideband power is absorbed in the critically coupled resonator.

The dependence of the power of the pump radiation leaving the critically coupled resonator is presented in Fig. 3. The dashed line stands for the transmission of the resonator for the pump light in the case of no oscillations excited (trivial solution), $|\langle B_{\pm}\rangle| = 0$. The solid line shows the region where oscillations can be excited. In that region the solution depicted by the dashed line is not stable because sidebands start to grow from fluctuations taking power from the pump light. Only the section of solid curve located between point *A* and *B* corresponds to the stable oscillations.

The dependencies of the maximum power of the generated sidebands and the corresponding optimum tuning of the pump laser frequency on the pump power are shown in Fig.

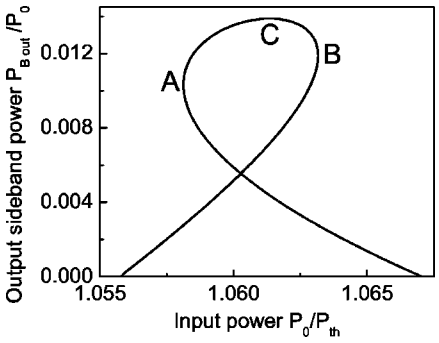

FIG. 2. Dependence of the sideband power on the input pump power for the case of identical resonator modes and pump frequency such that $\omega_0-\omega+\kappa(T)=1.8(\gamma_0+\gamma_{c0})$ $(\gamma_0=\gamma_{c0})$. Stable oscillations occur in the region between points *A* and *B* (point *C* shows the center of the region).

4 for the case of an overcoupled resonator. The value of the optimum detuning increases with the pump power to compensate for the power-dependent phase mismatch arising from the cross-phase modulation effect [2]. This mismatch

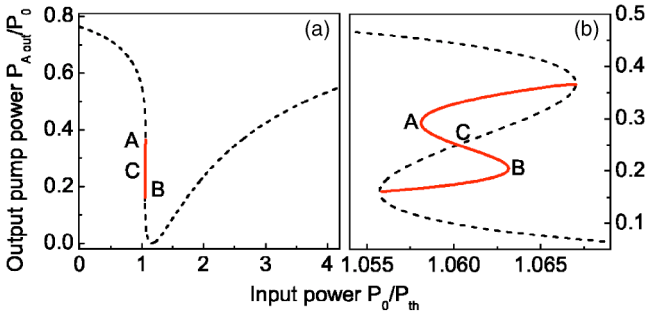

FIG. 3. Dependence of the pump power on the input pump power for the case of identical resonator modes and pump frequency such that $\omega_0-\omega+\kappa(T)=1.8(\gamma_0+\gamma_{c0})$. Stable oscillations occur in the region between points *A* and *B* (point *C* shows the center of the region). The dashed line shows the response of the system with no oscillations excited. (b) stands for the details of the pump power dependence in the stability region.

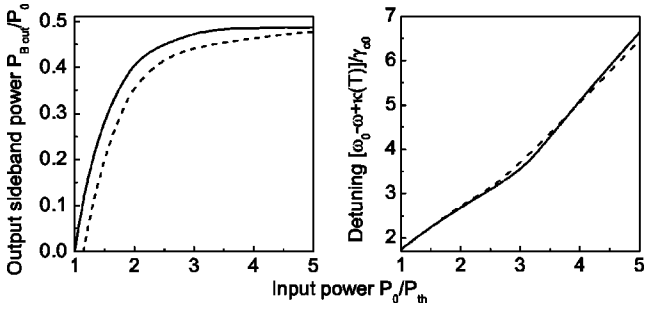

FIG. 4. Optimum sideband power (left) achieved at the optimum detuning of the pump laser frequency (right) versus the input pump power for the case of identical modes of an overcoupled resonator. Solid line stands for a resonator with no dispersion $(D=0)$, dashed line stands for the resonator with nonzero dispersion $(D=0.3)$. It is easy to see that at sufficiently large optical pump power and optimum pumping frequency complete redistribution of the pump power into sidebands is possible.

results from the different frequency spaces between one sideband and the pump, and the pump and the other sideband [see the second terms in the right-hand side of Eqs. (1)–(3)].

We considered only three interacting modes in the model, however, experiments show that a larger number of modes could participate in the process [13,14]. Those modes could change the efficiency curve (Fig. 4) rather significantly. The number of participating modes is limited by the nonequidistance of the modes of the resonator. Generally, modes of a resonator are not equidistant because of the second-order dispersion of the material and the geometrical dispersion given by the mode structure. We introduce $D=(2\omega_0-\omega_+-\omega_-)/\gamma_0$ to take the second-order dispersion of the resonator into account. If $|D|\geqslant 1$ the modes of the resonator are essentially not equidistant and therefore multiple harmonic generation is not possible.

Geometrical dispersion for the main mode sequence of a WGM resonator is $D\simeq 0.41c/(\gamma_0 R n_0 m^{5/3})$ [20,21], for a resonator with radius R; ω_+, ω_0, and ω_- are assumed to be $m+1$, m, and $m-1$ modes of the resonator $(\omega_m R n_{\omega_m}=mc,\ m\gg 1)$. For $R=0.4$ cm, $\gamma_0=2\times 10^5$ rad/s, $m=3\times 10^4$ we obtain $D=7\times 10^{-4}$, therefore the geometrical dispersion is relatively small. However, the dispersion of the material can be large enough. For instance, using Sellmeier's dispersion equation for CaF_2 we find $D\simeq 0.1$ at 1.3-μm laser wavelength. This implies that approximately three sideband pairs can be generated in the system. For small resonators geometrical dispersion could greatly exceed the material dispersion.

Let us now discuss the phase between generated sidebands, and the influence of this phase on the power of the signal generated on a photodiode that absorbs both the carrier and sidebands. The average power at the beat-note frequency $(\omega_+-\omega_-)/2$ is equal to

$$P_{mw}=2\mathcal{R}^2\rho|A^*_{out}B_{+\,out}+B^*_{-\,out}A_{out}|^2, \tag{11}$$

where A_{out} and $B_{\pm\,out}$ are to be found from Eqs. (7) and (8), $\mathcal{R}$ is a transformation coefficient of the optical power to a photocurrent, and ρ is the resistance at the output of the photodiode. The typical values are $\mathcal{R}=0.7$A/V, and $\rho=50\Omega$.

It is convenient to introduce parameter Φ, describing the relative phase between generated sidebands:

$$\Phi=\frac{|A^*_{out}B_{+\,out}+B^*_{-\,out}A_{out}|^2}{(|A^*_{out}B_{+\,out}|+|B^*_{-\,out}A_{out}|)^2}. \tag{12}$$

If $\Phi=0$, the phases of the sidebands are π-shifted with respect to each other and the light produced in the FWM process is phase modulated. In the opposite case, when $\Phi=1$, the light is amplitude modulated. We found that for the overcoupled resonator the signal is mostly phase modulated, while for the critically coupled resonator it is mostly amplitude modulated (Fig. 5).

IV. SOLUTION: PHASE DIFFUSION

Let us present the slow amplitudes of the field as

$$A=(|\langle A\rangle|+\delta A)e^{i(\phi_0+\delta\phi_0)}, \tag{13}$$

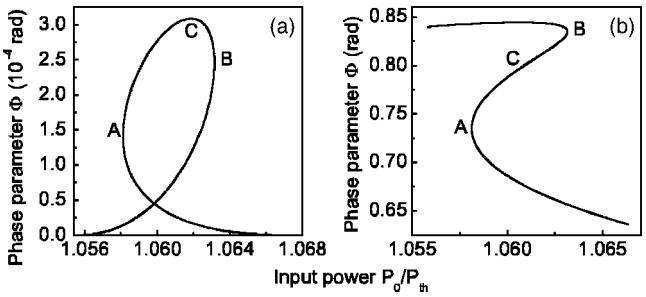

FIG. 5. Phase parameter Φ for overloaded (a) and critically loaded (b) resonators. All parameters coincide with parameters used in Figs. 1–3.

$$B_+ = (|\langle B_+\rangle| + \delta B_+)e^{i(\phi_+ + \delta\phi_+)}, \tag{14}$$

$$B_- = (|\langle B_-\rangle| + \delta B_-)e^{i(\phi_- + \delta\phi_-)}, \tag{15}$$

where δA, δB_+, and δB_- stand for the amplitude fluctuations of the fields, and $\delta\phi_0$, $\delta\phi_+$, and $\delta\phi_-$ stand for the phase fluctuations of the fields. For the sake of simplicity we consider the case of identical modes, when $|\langle B_+\rangle| = |\langle B_-\rangle| = |\langle B\rangle|$.

Using such a decomposition we obtain linearized differential equations for the fluctuations (see Appendix C). Solution of these equation allows us to find phase diffusion for the beat-note signal, proportional to $A^*_{out}B_{+\,out} + B^*_{-\,out}A_{out}$, as well as to study the stability of the oscillations.

The phase diffusion coefficient of the beat-note signal could be estimated from

$$D_{mw} = \left\{1 + \left[1.54\frac{P_{B\,out}}{P_{th}}\left(\frac{\gamma_0 + \gamma_{c0}}{2\gamma_{c0}}\right)^2\right]^2\right\} \times \frac{(\gamma_{c0} + \gamma_0)^2}{4}\frac{\hbar\omega_0}{P_{B\,out}}, \tag{16}$$

where $P_{B\,out}$ is the output power of a sideband. This expression is valid for the oscillations not far from the oscillation threshold. The expression could be optimized at

$$P_{B\,opt} = \frac{P_{th}}{1.54}\left(\frac{2\gamma_{c0}}{\gamma_0 + \gamma_{c0}}\right)^2. \tag{17}$$

The minimum phase diffusion coefficient is

$$D_{min} = \frac{(\gamma_{c0} + \gamma_0)^2}{2}\frac{\hbar\omega}{P_{B\,opt}} = \omega_0^2\frac{\gamma_0 + \gamma_{c0}}{2\gamma_{c0}}\frac{\hbar\omega_0 n_2\lambda}{4\pi\mathcal{V}n_0^2}. \tag{18}$$

The minimum phase diffusion does not depend on the parameters of the resonator except its volume. It is interesting to note that the oscillations are more stable for larger resonators (larger mode volumes $\mathcal{V}$).

The Allan deviation indicating the stability of the generated beat-note signal (at microwave frequency for larger resonators) is $\sigma_{beat}/\omega_{beat} = (2D_{mw}/t\omega_{beat}^2)^{1/2}$. We could estimate $\sigma_{beat}/\omega_{beat} \simeq 6\times10^{-14}/\sqrt{t}$ for $\omega_0 \simeq \omega = 1.4\times10^{15}$ rad/s, $\omega_{beat} = 5\times10^{10}$ rad/s, and $\gamma_0 = \gamma_{c0}$. The resonator temperature should be properly stabilized to achieve the estimated stability.

V. DISCUSSION

It is easy to see from Eq. (10) that the efficiency of the hyperparametric process increases with a decrease of the mode volume. Reducing the size of the resonator could result in a dramatic reduction of the threshold for the oscillation. Since the mode volume may be roughly estimated as $\mathcal{V} \approx 2\pi\lambda R^2$, it is clear that reducing the radius R by an order of magnitude would result in two orders of magnitude reduction in the threshold of the parametric process. This could place WGM resonators in the same class as the oscillators based on atomic coherence [9]. However, unlike the frequency difference between sidebands in the atomic oscillator, the frequency of the WGM oscillator could be free from power (ac Stark) shifts and the stability of the microwave beat-note signal generated in the process increases with the oscillation threshold increase (18).

The oscillations in nonlinear media could be masked with stimulated Raman scattering (SRS) and other nonlinear effects. This is also expected and observed in WGM resonators. For instance, the threshold for the SRS process in a WGM resonator may be estimated from [22]

$$P_R \simeq \frac{\pi^2 n_0^2 \mathcal{V}}{G\lambda^2 Q^2}, \tag{19}$$

where G is the Raman gain coefficient. For fused silica and some transparent crystals $G \simeq 10^{-11}$ cm/W. Comparing Eqs. (10) and (19) we estimate $P_{th}/P_R \approx 1$.

Hence an observation of secondary lines in the vicinity of the optical pumping line in the SRS experiments with WGM silica microresonators was interpreted as four-wave mixing between the pump and two Raman waves generated in the resonator, rather than as the four-photon parametric process based on electronic Kerr nonlinearity of the medium [22]. An interplay among various stimulated nonlinear processes has also been observed and studied in droplet spherical microcavities [23]. Therefore additional studies of the effects are important and crystalline WGM resonators could be helpful here. In contrast with resonators fabricated with amorphous materials and liquids, high-Q crystalline resonators would allow a better discrimination of the third-order nonlinear processes and the observation of pure hyperparametric oscillation signals because of additional selection rules imposed by the crystal symmetry.

Generally, pushing Q factors of WGM resonators higher would result in ultimate similarities between properties of atoms, quantum dots, and the resonator modes. For example, for very high-Q microresonators the material dispersion results in significantly nonequidistant mode spectrum. This spectrum would create an effective "two-level" system within the resonator. Strong confinement of the light in the resonator along with high Q factors would result in initializing efficient nonlinear processes on low light levels even with small nonlinearities of optically transparent materials. High efficiency controllable light coupling to the resonator modes [11] would allow integrating the resonators to optical fiber networks.

VI. CONCLUSION

We have theoretically studied properties of optical hyperparametric oscillations in a high-Q whispering-gallery-mode resonator. Due to the long interaction times of the pumping light with the material, even the small cubic nonlinearity of the material results in an efficient low-threshold generation of optical sidebands. Beat-note signal between the sidebands and the pump is characterized with a slow phase diffusion independent of the phase diffusion of the pumping laser. This process can be used for the demonstration of a different kind of an all-optical frequency reference.

ACKNOWLEDGMENTS

The research described in this paper was carried out by the Jet Propulsion Laboratory, California Institute of Technology, under a contract with the National Aeronautics and Space Administration, and with support from the DARPA AOSP Program.

APPENDIX A: HAMILTONIAN AND BASIC EQUATIONS

The Hamiltonian describing the system of three modes interacting by means of cubic nonlinearity is

$$H = H_0 + V, \quad H_0 = \hbar\omega_0 a^\dagger a + \hbar\omega_+ b_+^\dagger b_+ + \hbar\omega_- b_-^\dagger b_-,$$

$$V = -\hbar\frac{g}{2}(a^\dagger a^\dagger aa + b_+^\dagger b_+^\dagger b_+ b_+ + b_-^\dagger b_-^\dagger b_- b_-) - 2\hbar g(b_-^\dagger b_+^\dagger b_+ b_- + a^\dagger b_+^\dagger b_+ a + a^\dagger b_-^\dagger b_- a) - \hbar g(b_-^\dagger b_+^\dagger aa + a^\dagger a^\dagger b_+ b_-), \quad \text{(A1)}$$

where ω_0, ω_+, and ω_- are the eigenfrequencies of the optical cavity modes, a, b_+, and b_- are the annihilation operators for these modes, respectively, g is the coupling constant [see Eq. (5)]. Deriving this coupling constant we assume that (i) the index of refraction of the material can be presented in the form $n=n_0+n_2I$, where I denotes the time-average intensity of the field; (ii) the modes are nearly overlapped geometrically, which is true if the frequency difference between them is small.

The interaction part of the Hamiltonian is found from usual Kerr Hamiltonian $V=-\hbar(g/2):(a+b_++b_-+\text{H.c.})^4:$, where ": ⋯ :" means normal ordering, with application of rotating wave approximation. The simplified interaction Hamiltonian contains three terms responsible for self-phase modulation, cross-phase modulation, and four-wave mixing. This simple model is valid for media with nonresonant electronic nonlinearities, e.g., some transparent crystals and fused silica [24,25]. The sign of the interaction part is derived from expression for a mode resonant frequency $\omega_m \approx mc/(Rn)$ and the definition of the nonlinear index of refraction. It is important to note that the self- and cross-phase modulation terms of the Hamiltonian have the same order of magnitude as the four-wave mixing term and hence they influence significantly the oscillations in the system.

Using Hamiltonian (A1) we derive equations of motion for the field operators,

$$\dot{a} = -i\omega_0 a + ig[a^\dagger a + 2b_+^\dagger b_+ + 2b_-^\dagger b_-]a + 2iga^\dagger b_+ b_-, \quad \text{(A2)}$$

$$\dot{b}_+ = -i\omega_+ b_+ + ig[2a^\dagger a + b_+^\dagger b_+ + 2b_-^\dagger b_-]b_+ + igb_-^\dagger aa, \quad \text{(A3)}$$

$$\dot{b}_- = i\omega_- b_- + ig[2a^\dagger a + 2b_+^\dagger b_+ + b_-^\dagger b_-]b_- + igb_+^\dagger aa. \quad \text{(A4)}$$

This set of equation describes unitary evolution of the lossless system. We consider an open system. To describe the open system we introduce decay terms as well as Langevin fluctuation forces. Moreover, we have to take into account frequency shift due to temperature change of the resonator. Set (A2)–(A4) transforms to

$$\dot{a} = -[i\omega_0 + i\kappa_0(T) + \gamma_0 + \gamma_{c0}]a + ig[a^\dagger a + 2b_+^\dagger b_+ + 2b_-^\dagger b_-]a + 2iga^\dagger b_+ b_- + f_0 + f_{c0}, \quad \text{(A5)}$$

$$\dot{b}_+ = -[i\omega_+ + i\kappa_+(T) + \gamma_+ + \gamma_{c+}]b_+ + ig[2a^\dagger a + b_+^\dagger b_+ + 2b_-^\dagger b_-]b_+ + igb_-^\dagger aa + f_+ + f_{c+}, \quad \text{(A6)}$$

$$\dot{b}_- = -[i\omega_- + i\kappa_-(T) + \gamma_- + \gamma_{c-}]b_- + ig[2a^\dagger a + 2b_+^\dagger b_+ + b_-^\dagger b_-]b_- + igb_+^\dagger aa + f_- + f_{c-}. \quad \text{(A7)}$$

The Langevin forces are described by the following nonvanishing commutation relations:

$$[f_0(t), f_0^\dagger(t')] = 2\gamma_0\delta(t-t'), \quad [f_+(t), f_+^\dagger(t')] = 2\gamma_+\delta(t-t'),$$

$$[f_-(t), f_-^\dagger(t')] = 2\gamma_-\delta(t-t'), \quad [f_{c0}(t), f_{c0}^\dagger(t')] = 2\gamma_{c0}\delta(t-t'),$$

$$[f_{c+}(t), f_{c+}^\dagger(t')] = 2\gamma_{c+}\delta(t-t'), [f_{c-}(t), f_{c-}^\dagger(t')] = 2\gamma_{c-}\delta(t-t'), \quad \text{(A8)}$$

and average values

$$\langle f_{c0}\rangle = \sqrt{\frac{2\gamma_{c0}P_0}{\hbar\omega_0}}\, e^{-i\omega t}, \quad \langle f_+\rangle = \langle f_-\rangle = \langle f_{c+}\rangle = \langle f_{c-}\rangle = \langle f_c\rangle = 0, \quad \text{(A9)}$$

where P_0 is the pump power of the mode. We assume that the fluctuations entering each mode are in the coherent state and are uncorrelated with each other.

Let us introduce now slowly varying amplitudes for the mode operators as follows:

$$a = Ae^{-i\omega t}, b_+ = B_+e^{-i\tilde{\omega}_+ t}, \hat{b} - = B_-e^{-i\tilde{\omega}_- t}, \quad \text{(A10)}$$

where ω is the carrier frequency of the external pump of the mode a, $\tilde{\omega}_+$ and $\tilde{\omega}_-$ are the frequencies of modes b_+ and b_-, respectively. Those frequencies obey ratio (4). Then from Eqs. (A2)–(A4) it is easy to derive Eqs. (1)–(3) for the slow amplitudes of the intracavity fields. This is the basic set of equations we are going to analyze. It is worth noting that this set has a lot in common with the set of coupled wave equations derived for light propagation in optical fibers [3,26,27] and atoms in a cavity [28].

APPENDIX B: STEADY-STATE SOLUTION OF EQS. (1)–(3) FOR EXPECTATION VALUES

Let us solve set (1)–(3) in steady state keeping expectation values only,

$$\Gamma_0\langle A\rangle = ig[|\langle A\rangle|^2 + 2|\langle B_+\rangle|^2 + 2|\langle B_-\rangle|^2]\langle A\rangle + 2ig\langle A^*\rangle\langle B_+\rangle\langle B_-\rangle + \langle F_{c0}\rangle, \tag{B1}$$

$$\Gamma_+\langle B_+\rangle = ig(2|\langle A\rangle|^2 + 2|\langle B_-\rangle|^2 + |\langle B_+\rangle|^2)\langle B_+\rangle + ig\langle B_-^*\rangle\langle A\rangle^2, \tag{B2}$$

$$\Gamma_-\langle B_-\rangle = ig(2|\langle A\rangle|^2 + |\langle B_-\rangle|^2 + 2|\langle B_+\rangle|^2)\langle B_-\rangle + ig\langle B_+^*\rangle\langle A\rangle^2. \tag{B3}$$

It is convenient to introduce combined decay rates for the modes as $\overline{\gamma}_j=\gamma_j+\gamma_{cj}$, and to rewrite Eqs. (B1)–(B3) as well as Eq. (4) with respect to dimensionless variables $\xi = g|\langle A\rangle|^2/\overline{\gamma}_0$ where $\langle A\rangle=|\langle A\rangle|\exp i\phi_0$; $\mathcal{B}_+=|\langle B_+\rangle|/|\langle A\rangle|$ where $\langle B_+\rangle=|\langle B_+\rangle|\exp i\phi_+$; $\mathcal{B}_-=|\langle B_-\rangle|/|\langle A\rangle|$ where $\langle B_-\rangle =|\langle B_-\rangle|\exp i\phi_-$; $\psi=\phi_{F_{c0}}-\phi_0$ where $\langle F_{c0}\rangle=|\langle F_{c0}\rangle|\exp i\phi_{F_{c0}}$; $\phi=2\phi_0-\phi_+-\phi_-$; $\Delta_+=[\omega_+-\tilde{\omega}_+ +\kappa(T)]/\overline{\gamma}_0$; and $\Delta_-=[\omega_- -\tilde{\omega}_- +\kappa(T)]/\overline{\gamma}_0$. The pumping force can be conveniently transformed to a dimensionless value $f=(g/\overline{\gamma}_0)^{1/2}|\langle F_{c0}\rangle|/\overline{\gamma}_0$; dimensionless drive detuning can be introduced $\Delta_0=[\omega_0-\omega +\kappa(T)]/\overline{\gamma}_0$ as well. We assume that the temperature is stabilized such that it is possible to neglect by the temperature modification of the resonator FSR, so all κ_i are identical and equal to κ.

Generally, modes of a resonator are not equidistant because of the second-order dispersion of the material as well as geometrical dispersion given by the mode structure. To take the second-order dispersion of the resonator into account we introduce $D=(2\omega_0-\omega_+-\omega_-)/\overline{\gamma}_0\simeq\beta''/(\overline{\gamma}_0R^2\beta'^3)$, where β' and β'' come from the dispersion relation

$$\frac{\omega}{c}n(\omega)\simeq\frac{\omega_0}{c}n_0+\beta'(\omega-\omega_0)+\frac{1}{2}\beta''(\omega-\omega_0)^2$$

for the resonator of radius R; and ω_+, ω_0, and ω_- are assumed to be $m+1$, m, and $m-1$ modes of the resonator ($\omega_m Rn_{\omega_m}=mc$, $m\gg 1$).

Finally, we arrive at

$$\sqrt{\xi}(1-2\xi\mathcal{B}_+\mathcal{B}_-\sin\phi)=f\cos\psi, \tag{B4}$$

$$\sqrt{\xi}\{\Delta_0-\xi[1+2(\mathcal{B}_+^2+\mathcal{B}_-^2+\mathcal{B}_+\mathcal{B}_-\cos\phi)]\}=f\sin\psi, \tag{B5}$$

$$\overline{\gamma}_+\mathcal{B}_+ +\overline{\gamma}_0\xi\mathcal{B}_-\sin\phi=0, \tag{B6}$$

$$[\Delta_+-\xi(2+\mathcal{B}_+^2+2\mathcal{B}_-^2)]\mathcal{B}_+-\xi\mathcal{B}_-\cos\phi=0, \tag{B7}$$

$$\overline{\gamma}_-\mathcal{B}_- +\overline{\gamma}_0\xi\mathcal{B}_+\sin\phi=0, \tag{B8}$$

$$[\Delta_--\xi(2+\mathcal{B}_+^2+2\mathcal{B}_-^2)]\mathcal{B}_--\xi\mathcal{B}_+\cos\phi=0, \tag{B9}$$

$$\Delta_++\Delta_-=2\Delta_0-D. \tag{B10}$$

Eqations (B6)–(B10) allow us to find parameters ξ, ϕ, Δ_+, Δ_- as well as a ratio between $\mathcal{B}_+$ and $\mathcal{B}_-$:

$$\xi^2=\frac{\overline{\gamma}_+\overline{\gamma}_-}{\overline{\gamma}_0^2}+\frac{\overline{\gamma}_+\overline{\gamma}_-}{(\overline{\gamma}_++\overline{\gamma}_-)^2}\{2\Delta_0-D-\xi[4+3(\mathcal{B}_+^2+\mathcal{B}_-^2)]\}^2, \tag{B11}$$

$$\sin\phi=-\frac{\sqrt{\overline{\gamma}_+\overline{\gamma}_-}}{\overline{\gamma}_0\xi}, \tag{B12}$$

$$\cos\phi=\frac{\{2\Delta_0-D-\xi[4+3(\mathcal{B}_+^2+\mathcal{B}_-^2)]\}\sqrt{\overline{\gamma}_+\overline{\gamma}_-}}{(\overline{\gamma}_++\overline{\gamma}_-)\xi}, \tag{B13}$$

$$\Delta_+=(2\Delta_0-D)\frac{\overline{\gamma}_+}{\overline{\gamma}_-+\overline{\gamma}_+}+\xi(2+\mathcal{B}_+^2+\mathcal{B}_-^2)\frac{\overline{\gamma}_--\overline{\gamma}_+}{\overline{\gamma}_-+\overline{\gamma}_+}+\xi(\overline{\gamma}_-\mathcal{B}_-^2-\overline{\gamma}_+\mathcal{B}_+^2), \tag{B14}$$

$$\Delta_-=(2\Delta_0-D)\frac{\overline{\gamma}_-}{\overline{\gamma}_-+\overline{\gamma}_+}-\xi(2+\mathcal{B}_+^2+\mathcal{B}_-^2)\frac{\overline{\gamma}_--\overline{\gamma}_+}{\overline{\gamma}_-+\overline{\gamma}_+}-\xi(\overline{\gamma}_-\mathcal{B}_-^2-\overline{\gamma}_+\mathcal{B}_+^2), \tag{B15}$$

$$\frac{\mathcal{B}+}{\mathcal{B}-}=\sqrt{\frac{\overline{\gamma}_-}{\overline{\gamma}_+}}. \tag{B16}$$

Now, from Eqs. (B4) and (B5) we find ψ and, say, B_-:

$$\left[1+2\frac{\overline{\gamma}_-}{\overline{\gamma}_0}\mathcal{B}_-^2\right]^2+\left[\Delta_0-\xi-2\xi\mathcal{B}_-^2\left(\frac{(\overline{\gamma}_--\overline{\gamma}_+)^2}{\overline{\gamma}_+(\overline{\gamma}_++\overline{\gamma}_-)}+\frac{\overline{\gamma}_-(2\Delta_0-D)}{\xi(\overline{\gamma}_++\overline{\gamma}_-)}-3\frac{\overline{\gamma}_-}{\overline{\gamma}_+}\mathcal{B}_-^2\right)\right]^2=\frac{f^2}{\xi}, \tag{B17}$$

$$\cos\psi=\frac{\sqrt{\xi}}{f}\left[1+2\frac{\overline{\gamma}_-}{\overline{\gamma}_0}\mathcal{B}_-^2\right], \tag{B18}$$

$$\sin\psi=\frac{\sqrt{\xi}}{f}\left[\Delta_0-\xi-2\xi\mathcal{B}_-^2\left(\frac{(\overline{\gamma}_--\overline{\gamma}_+)^2}{\overline{\gamma}_+(\overline{\gamma}_++\overline{\gamma}_-)}+\frac{\overline{\gamma}_-(2\Delta_0-D)}{\xi(\overline{\gamma}_++\overline{\gamma}_-)}-3\frac{\overline{\gamma}_-}{\overline{\gamma}_+}\mathcal{B}_-^2\right)\right]. \tag{B19}$$

To simplify analysis of the set of equations it is convenient to assume that $\overline{\gamma}_+=\overline{\gamma}_-=\overline{\gamma}_0$. This assumption is justified by the fact that identical, closely separated in frequency, modes of a resonator have identical Q factors. Then $\mathcal{B}_+=\mathcal{B}_-=\mathcal{B}$. Equations (B14) and (B15) transform to Eq. (9). The oscillation amplitude is determined by Eqs. (B11) and (B17), that could be rewritten in the form

$$4(\xi^2-1)-(2\Delta_0-D-6\xi\mathcal{B}^2-4\xi)^2=0, \tag{B20}$$

$$\xi\{(1+2\mathcal{B}^2)^2+[\Delta_0-\xi-\mathcal{B}^2(2\Delta_0-D-6\xi\mathcal{B}^2)]^2\}=f^2. \tag{B21}$$

From Eq. (B20) we get

$$\Delta_0 = 2\xi \pm \sqrt{\xi^2 - 1} + \frac{D}{2} + 3\xi\mathcal{B}^2. \tag{B22}$$

The external pump power with which Eqs. (B20) and (B21) and have a nontrivial solution approaches its smallest possible value (oscillation threshold) when the laser frequency is determined by the "−" sign in Eq. (B22). The threshold conditions (assuming $D=0$) are

$$\xi \simeq 1.175, \tag{B23}$$

$$\Delta_0 \simeq 1.733, \tag{B24}$$

$$f \simeq 1.24. \tag{B25}$$

Equation (B25) can be rewritten with respect to the pump power [see Eq. (10)].

To find microwave power generated on a photodiode we rewrite Eq. (11) in the form

$$P_{mw} = 2\mathcal{R}^2\rho P_0^2 \frac{4\gamma_{c0}^2}{\bar{\gamma}_0^2}\frac{\xi\mathcal{B}^2}{f^2}\left|\left(\frac{2\gamma_{c0}}{\bar{\gamma}_0}\frac{\sqrt{\xi}}{f} - e^{-i\psi}\right) + e^{i\phi}\left(\frac{2\gamma_{c0}}{\bar{\gamma}_0}\frac{\sqrt{\xi}}{f} - e^{-i\psi}\right)\right|^2, \tag{B26}$$

where we used the relations

$$\left(\frac{2\gamma_{c0}|\langle B_\pm\rangle|}{|\langle F_{c0}\rangle|}\right)^2 = \frac{4\gamma_{c0}^2}{\bar{\gamma}_0^2} = \frac{\xi\mathcal{B}^2}{f^2}, \qquad \left|\frac{2\gamma_{c0}}{\bar{\gamma}_0}\frac{\sqrt{\xi}}{f} - e^{-i\psi}\right|^2 = \frac{P_{A\,out}}{P_0}. \tag{B27}$$

APPENDIX C: STEADY-STATE SOLUTION OF EQS. (1)–(3) FOR FLUCTUATIONS—STABILITY ANALYSIS AND FREQUENCY DRIFT

Substituting Eqs. (13)–(15) into Eqs. (1)–(3), and introducing $\bar{F}_j = F_{cj} + F_j$, we derive a set of equations for the amplitude fluctuations,

$$\delta\dot{A} = -\frac{|\langle F_{c0}\rangle|}{|\langle A\rangle|}\cos\psi\ \delta A + 2g|\langle A\rangle||\langle B\rangle|^2\cos\phi\ \delta\phi + |\langle F_{c0}\rangle|\sin\psi\ \delta\phi_0 + 2g|\langle A\rangle||\langle B\rangle|\sin\phi\ (\delta B_- + \delta B_+) + \frac{1}{2}[(\bar{F}_0 - \langle F_{c0}\rangle)e^{-i\phi_0} + \text{H.c.}], \tag{C1}$$

$$\delta\dot{B}_+ = -g|\langle A\rangle|\sin\phi\,[2|\langle B\rangle|\delta A + |\langle A\rangle|(\delta B_- - \delta B_+)] - g|\langle A\rangle|^2|\langle B\rangle|\cos\phi\ \delta\phi + \frac{1}{2}(\bar{F}_+ e^{-i\phi_+} + \text{H.c.}), \tag{C2}$$

$$\delta\dot{B}_- = -g|\langle A\rangle|\sin\phi\,[2|\langle B\rangle|\delta A - |\langle A\rangle|(\delta B_- - \delta B_+)] - g|\langle A\rangle|^2|\langle B\rangle|\cos\phi\ \delta\phi + \frac{1}{2}(\bar{F}_- e^{-i\phi_-} + \text{H.c.}) \tag{C3}$$

and phase fluctuations

$$\delta\dot{\phi}_0 = \left(2g|\langle A\rangle|^2 - \frac{|\langle F_{c0}\rangle|}{|\langle A\rangle|}\sin\psi\right)\frac{\delta A}{|\langle A\rangle|} - \frac{|\langle F_{c0}\rangle|}{|\langle A\rangle|}\cos\psi\ \delta\phi_0 + 2g|\langle B\rangle|(2+\cos\phi)(\delta B_- + \delta B_+) - 2g|\langle B\rangle|^2\sin\phi\ \delta\phi + \frac{(\bar{F}_0 - \langle F_{c0}\rangle)e^{-i\phi_0} - \text{H.c.}}{2i|\langle A\rangle|}, \tag{C4}$$

$$\delta\dot{\phi}_+ = 2g|\langle A\rangle|\left[2\delta A + \frac{|\langle B\rangle|}{|\langle A\rangle|}(2\delta B_- + \delta B_+)\right] + g|\langle A\rangle|\cos\phi\left[2\delta A + \frac{|\langle A\rangle|}{|\langle B\rangle|}(\delta B_- - \delta B_+)\right] - g|\langle A\rangle|^2\sin\phi\ \delta\phi + \frac{\bar{F}_+ e^{-i\phi_+} - \text{H.c.}}{2i|\langle B\rangle|}, \tag{C5}$$

$$\delta\dot{\phi}_- = 2g|\langle A\rangle|\left[2\delta A + \frac{|\langle B\rangle|}{|\langle A\rangle|}(2\delta B_+ + \delta B_-)\right] + g|\langle A\rangle|\cos\phi\left[2\delta A - \frac{|\langle A\rangle|}{|\langle B\rangle|}(\delta B_- - \delta B_+)\right] - g|\langle A\rangle|^2\sin\phi\ \delta\phi + \frac{\bar{F}_- e^{-i\phi_-} - \text{H.c.}}{2i|\langle B\rangle|}. \tag{C6}$$

Using this set we derive two equation sets,

$$\delta\dot{A} = -\frac{|\langle F_{c0}\rangle|}{|\langle A\rangle|}\cos\psi\ \delta A + 2g|\langle A\rangle||\langle B\rangle|^2\cos\phi\ \delta\phi + |\langle F_{c0}\rangle|\sin\psi\ \delta\phi_0 + 2g|\langle A\rangle||\langle B\rangle|\sin\phi\ (\delta B_- + \delta B_+) + \frac{1}{2}((\bar{F}_0 - \langle F_{c0}\rangle)e^{-i\phi_0} + \text{H.c.}), \tag{C7}$$

$$\delta\dot{\phi}_0 = \left(2g|\langle A\rangle|^2 - \frac{|\langle F_{c0}\rangle|}{|\langle A\rangle|}\sin\psi\right)\frac{\delta A}{|\langle A\rangle|} - \frac{|\langle F_{c0}\rangle|}{|\langle A\rangle|}\cos\psi\ \delta\phi_0 + 2g|\langle B\rangle|(2+\cos\phi)(\delta B_- + \delta B_+) - 2g|\langle B\rangle|^2\sin\phi\ \delta\phi + \frac{(\bar{F}_0 - \langle F_{c0}\rangle)e^{-i\phi_0} - \text{H.c.}}{2i|\langle A\rangle|}, \tag{C8}$$

$$\delta\dot{B}_+ + \delta\dot{B}_- = -4g|\langle A\rangle||\langle B\rangle|\sin\phi\ \delta A - 2g|\langle B\rangle||\langle A\rangle|^2\cos\phi\ \delta\phi + \frac{1}{2}(\bar{F}_+ e^{-i\phi_+} + \bar{F}_- e^{-i\phi_-} + \text{H.c.}), \tag{C9}$$

$$\delta\dot{\phi} = -2\left[2g|\langle A\rangle|^2(1+\cos\phi) + \frac{|\langle F_{c0}\rangle|}{|\langle A\rangle|}\sin\psi\right]\frac{\delta A}{|\langle A\rangle|} - 2\frac{|\langle F_{c0}\rangle|}{|\langle A\rangle|}\cos\psi\ \delta\phi_0 + 2g|\langle B\rangle|(1+2\cos\phi)(\delta B_- + \delta B_+) + 2g\sin\phi\ (|\langle A\rangle|^2 - 2|\langle B\rangle|^2)\delta\phi + \frac{(\bar{F}_0 - \langle F_{c0}\rangle)e^{-i\phi_0} - \text{H.c.}}{i|\langle A\rangle|}$$

$$-\frac{\bar{F}_+e^{-i\phi_+}-\text{H.c.}}{2i|\langle B\rangle|}-\frac{\bar{F}_-e^{-i\phi_-}-\text{H.c.}}{2i|\langle B\rangle|}, \tag{C10}$$

and

$$\delta\dot{\phi}_+-\delta\dot{\phi}_-=2g(|\langle A\rangle|^2\cos\phi\ +|\langle B\rangle|^2)\frac{\delta B_--\delta B_+}{|\langle B\rangle|}+\frac{1}{2i|\langle B\rangle|}(\bar{F}_+e^{-i\phi_+}-\bar{F}_-e^{-i\phi_-}-\text{H.c.}), \tag{C11}$$

$$\delta\dot{B}_--\delta\dot{B}_+=2g|\langle A\rangle|^2\sin\phi\ (\delta B_--\delta B_+)+\frac{1}{2}(\bar{F}_-e^{-i\phi_-}-\bar{F}_+e^{-i\phi_+}+\text{H.c.}), \tag{C12}$$

Using the first set we could study the stability of the oscillations. The second set of equations, always stable because $\sin\phi<0$, allows us to find the phase diffusion of the beat note generated in the process of adsorption of the pump and sidebands on a fast photodiode.

Keeping in mind that in the case of stable oscillations $\delta\dot{B}_--\delta\dot{B}_+=0$, we arrive at

$$\delta\dot{\phi}_+-\delta\dot{\phi}_-=\frac{|\langle A\rangle|^2\cos\phi+|\langle B\rangle|^2}{|\langle A\rangle|^2\sin\phi}\frac{\bar{F}_+e^{-i\phi_+}-\bar{F}_-e^{-i\phi_-}+\text{H.c.}}{2|\langle B\rangle|}\times\frac{\bar{F}_+e^{-i\phi_+}-\bar{F}_-e^{-i\phi_-}-\text{H.c.}}{2i|\langle B\rangle|} \tag{C13}$$

or, using the fact that the equation corresponding to the energy conservation law (4) can be derived in the case of long integration time for stable oscillations,

$$\delta\dot{\phi}=2\delta\dot{\phi}_0-\delta\dot{\phi}_+-\delta\dot{\phi}_-\simeq 0, \tag{C14}$$

we obtain

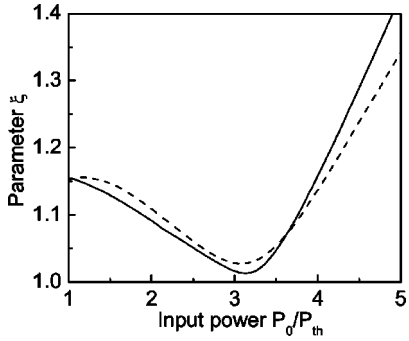

FIG. 6. Parameter ξ corresponding to the optimum sideb and power achieved at the optimum detuning of the pump laser frequency (see Fig. 4) versus the input pump power for the case of identical modes of an overcoupled resonator. The solid line st and s for a dispersionless resonator ($D=0$), the dashed line st and sfor the resonator with nonzero dispersion ($D=0.3$).

$$\delta\dot{\phi}_+-\delta\dot{\phi}_0=\delta\dot{\phi}_0-\delta\dot{\phi}_-=\frac{|\langle A\rangle|^2\cos\phi\ +|\langle B\rangle|^2}{|\langle A\rangle|^2\sin\phi}\frac{\bar{F}_+e^{-i\phi_+}-\bar{F}_-e^{-i\phi_-}+\text{H.c.}}{4|\langle B\rangle|}+\frac{\bar{F}_+e^{-i\phi_+}-\bar{F}_-e^{-i\phi_-}-\text{H.c.}}{4i|\langle B\rangle|}. \tag{C15}$$

Using expressions [see Eq. (B12)] $\sin\phi=-1/\xi$ and $\cos\phi=\pm\sqrt{\xi^2-1}/\xi$ we derive the expression for the diffusion coefficient for the beat note,

$$D_{mw}=\left[1+(\sqrt{\xi^2-1}\pm\xi\mathcal{B}^2)^2\right]\frac{\bar{\gamma}_0^2}{4}\frac{\hbar\omega_0}{P_{B\ out}}, \tag{C16}$$

resulting in Eq. (16) in the limit $\xi\approx 1$. This is a valid approximation. For instance, in the case of overcoupled resonator and optimum laser tuning (see Fig. 4) the parameter ξ has the power dependence depicted in Fig. 6.

[1] D. N. Klyshko, *Photons and Nonlinear Optics* (Taylor and Francis, New York, 1988).
[2] G. P. Agrawal, *Nonlinear Fiber Optics* (Academic Press, New York, 1995).
[3] R. H. Stolen and J. E. Bjorkholm, IEEE J. Quantum Electron. **QE-18**, 1062 (1982).
[4] S. Coen and M. Haelterman, Opt. Lett. **26**, 39 (2001).
[5] P. A. Roos, L. S. Meng, S. K. Murphy, and J. L. Carlsten, J. Opt. Soc. Am. B **21**, 357 (2004).
[6] D. Grandclement, G. Grynberg, and M. Pinard, Phys. Rev. Lett. **59**, 40 (1987).
[7] D. Grandclement, G. Grynberg, and M. Pinard, Phys. Rev. Lett. **59**, 44 (1987).
[8] G. Khitrova, J. F. Valley, and H. M. Gibbs, Phys. Rev. Lett. **60**, 1126 (1988).
[9] A. S. Zibrov, M. D. Lukin, and M. O. Scully, Phys. Rev. Lett. **83**, 4049 (1999).
[10] J. Vuckovic, M. Pelton, A. Scherer, and Y. Yamamoto, Phys. Rev. A **66**, 023808 (2002).
[11] K. J. Vahala, Nature (London) **424**, 839 (2003).
[12] C. Conti, A. Di Falco, and G. Assanto, Opt. Express **12**, 823 (2004).
[13] T. J. Kippenberg, S. M. Spillane, and K. J. Vahala, Phys. Rev. Lett. **93**, 083904 (2004).
[14] A. A. Savchenkov, A. B. Matsko, D. Strekalov, M. Mohageg, V. S. Ilchenko, and L. Maleki, Phys. Rev. Lett. **93**, 243905 (2004).
[15] A. A. Savchenkov, V. S. Ilchenko, A. B. Matsko, and L. Maleki, Phys. Rev. A **70**, 051804 (2004).
[16] M. L. Gorodetsky and V. S. Ilchenko, Laser Phys. **2**, 1004 (1992).
[17] A. E. Fomin, M. L. Gorodetsky, I. S. Grudinin, and V. S. Ilchenko, Proc. SPIE **5333**, 231 (2004).
[18] T. Carmon, L. Yang, and K. J. Vahala, Opt. Express **12**, 4742 (2004).
[19] M. Fleischhauer, M. D. Lukin, A. B. Matsko, and M. O.

Scully, Phys. Rev. Lett. **84**, 3558 (2000).
[20] V. S. Ilchenko, A. A. Savchenkov, A. B. Matsko, and L. Maleki, J. Opt. Soc. Am. A **20**, 157 (2003).
[21] L. Maleki, A. A. Savchenkov, V. S. Ilchenko, A. B. Matsko, Proc. SPIE **5104**, 1 (2003).
[22] S. M. Spillane, T. J. Kippenberg, and K. J. Vahala, Nature (London) **415**, 621 (2002).
[23] H.-B. Lin and A. J. Campillo, Phys. Rev. Lett. **73**, 2440 (1994).
[24] P. D. Maker and R. W. Terhune, Phys. Rev. **137**, A801 (1965).
[25] R. W. Boyd, *Nonlinear Optics* (Academic Press, New York, 1992).
[26] J. Bar-Joseph, A. A. Friesem, R. G. Waarts, and H. H. Yaffe, Opt. Lett. **11**, 534 (1986).
[27] G. Cappellini and S. Trillo, J. Opt. Soc. Am. B **8**, 824 (1991).
[28] M. Brambilla, F. Castelli, L. A. Lugiato, F. Prati, and G. Strini, Opt. Commun. **83**, 367 (1991).